International Journal of Engineering & Technology, 7 (3.28) (2018) 218-226

International Journal of Engineering & Technology

Website: www.sciencepubco.com/index.php/IJET

Research paper

Response Surface Methodology for Optimizing Giant Magneto-Resistive (GMR)-Bobbing Coil Probe for Carbon Steel Pipeline Crack Detection

Moneer A Faraj[1,2]*, Fahmi Samsuri[1], Ahmed N AbdAlla[3], Damhuji Rifai[4], Kharudin Ali[4], Y Al-Douri[5]

[1]*Faculty of Electrical and Electronics, Universiti Malaysia Pahang, Kuantan, Malaysia*
[2]*Electronics Engineering Department, Omar Al Mukhtar Universityal, Al Baida, Libya*
[3]*Faculty of Electronic and Information Eng, Huaiyin Institute of Technology, Huai'an 223002, Jiansu, China*
[4]*Faculty of Electrical and Automation Engineering Technology, TATI University College, Malaysia*
[5]*Nanotechnology and Catalysis Research Center (NANOCAT), University of Malaya, 50603 Kuala Lumpur, Malaysia*
**Corresponding author E-mail: mod84_91@yahoo.com*

Abstract

Inspection of inner wall cracks is critical in the evaluation of carbon steel pipe integrity. In this study, the optimization of Giant magneto-resistive (GMR)-Bobbing coil probe (GMR-BC) based eddy current technique for carbon steel pipeline was proposed. Bobbing coil was used in the magnetization of pipe and the GMR sensor array in the identification of field leakages from the pipe crack. Response surface methodology (RSM) was utilized to optimize the dimension which includes GMR sensors, height of the coil, and lift-off depending on the desirability technique. The efficiency of this approach was by estimating the change in the axial component of leakage flux from axial and hole defects artificially machined on the wall pipe. The results obtained experimentally were in good agreement with the predicted mathematical model using RSM in the prediction of axial and hole defect detection. The result reflected that 6 GMR sensors, 2 mm of lift-off, and 10 mm of coil height were the optimum conditions of GMR-BC probe that detected all the axial and hole defect in 60 mm carbon steel pipe.

Keywords: *Eddy Current Testing; Non-Destructive Testing; GMR Sensor; Defect Detection; Response surface methodology*.

1. Introduction

Eddy current testing (ECT) is a common method used for evaluating the integrity of pipelines. To avoid any form of catastrophic failure, it is imperative to identify the problems associated with the components at an initial stage [1]. Many NDT approaches are being employed in pipeline inspection, they include Magnetic Flux Leakage (MFL), Radiographic testing (RT), Eddy Current Testing (ECT), and Ultrasonic Testing (UT). UT approach can give an appropriate defect profile; this approach only needs a coupling in the transmission of a signal between the testing sample and probe [2]. In this case, ECT is preferred as an excellent non-destructive testing approach due to its high sensitivity, ease of operation, and versatility [3]. Overall, this approach can recognize the subsurface depth because of the eddy current exponential decay by adjusting the excitation current frequency. In addition, the inspection depth can be amended.

Despite the depth penetration of eddy currents is being enhanced by reducing the excitation frequency, the sensitivity detection of a coil is being limited by the magnetic field feeble strength in the subsurface defect [4, 5]. Therefore, using a higher responsive magnetic field sensor is important in measuring feeble magnetic fields in the flaws. The advantage of magnetometer (MR) sensors in relative to coil had been implemented to be the magnetic field detection approach in ECT probe. Using a Giant magneto resistance (GMR) sensor as the receiver has received more attention because of its higher detection for a feeble magnetic field, a wider range of frequency capacity, and an enormous spatial resolution [6].

The efficiency of the eddy current probe is mainly controlled through its basic design and operation mode. There are many studies and postulated methods used in the improvement of the probability of eddy current probe defect detection by selecting an optimal construction variable set. In [2] designed and implemented a giant magnetic resistance sensor array to inspect outer pipe wall defect. The obtained results showed that the design permits every part of the pipe to be examined and can detect various defects within the ferromagnetic pipe with good accuracy. In [7] utilized a GMR sensor array to identify defects and cracks in the seamless steel pipe. Cheng [8] used pulse eddy current with GMR sensor to determine the flaws in the walls of carbon steel pipes. The result approves that the eddy current system using a GMR sensor can detect a minor defect in the inner pipe. In [9] used a rotating magnetic field to induce the carbon steel pipe of 70 mm and six GMR sensors to identify the variation in a magnetic field; 1.5 x 13.5 x 5 mm^3 volume of defects were detected. In [10] used a TMR sensor to detect the crack in 12 mm thick SS400 steel plate in relation to width, depth, and length. The results showed that TMR sensors are good in the inspection of steel even at the tapered point where signal varies with a higher signal to noise ratio on the crack point. In [11] utilized eddy current coil and GMR sensor to extend the detection of flaws (> 5.0 mm) on 316 stainless steel plates of 8.0 mm thickness with subsurface and six surface notches. The magnetic fields induced over the flaws in 8.0 mm thick stainless-steel plates are dependably determined by utilizing the proposed integrated EC-GMR sensor.

However, depth evaluation of defect is affected by lift-off. In [12] proposed the method to inspect multilayer aluminium sheets (1.0 mm thick) by utilizing a GMR-based eddy current sensor in the detection of subsurface defects. In [13] used the GMR detection to evaluate the crack depth in a 4 mm thick aluminium plate. The results showed that there was a clear relationship between the peak's amplitudes and crack's depth. In [14] studied the influence of the thickness of rectangular winding, diameter, a height of coil and frequencies on the design of a rotating field eddy current probe with bobbin pick-up coil. The experimental results showed the maximizing defect detection probability which includes circumferential notches and axial in the wall tube by using the RoFEC probe with an optimum parameter. In [15] studied the influence of geometrical parameters on the spatial discrimination and probe response amplitude. The probe was manufactured with PCB technology. The results reflected that modified parameters in the study can significantly increase the performance of the probe. In [16] proposed a process in the determination of optimal variables of a sensor system to obtain higher accuracy in the reconstruction of the crack shapes. Computer-aided design tools have been used to design a sensor probe and the results indicated that the postulated sensor geometry enhanced the sensitivity of probe in relation to the depth variations in a crack. However, the optimization of probe design is still crucial in achieving high levels of reliability.

This study was carried out to characterize, design, and optimize different GMR-BC probe design using the design expert software in a bid to find the best design parameters. The bobbin coil was used to facilitate the eddy current in the test sample during the motion and series of GMR sensors to detect the variation in the magnetic field due to pipeline defect. The RSM used in the optimization of the number of GMR sensors, height of the coil, and lift-off played a critical role in designing the GMR-BC probe to increase the detection of axial and hole defects.

2. Related Work

2.1. The Parameters Affect the ECT Probes Performance

In recent year, many researchers have focused on designing EC probes for specified applications. The parameters design of EC probes was optimized to increase the resolution and sensitivity of the defect detection. The previous studies identify the parameters that affect the eddy current testing probe performance for increasing the capability of detection defect in the conductivity material as lift-off, height of coil, frequency, and detector sensors [11, 14, 17, 18]. Therefore, these parameters which include detector sensor, height of coil, and lift-off were selected in this current study to investigate the influence of probe design parameters on the accuracy of probe defect detection in 55 mm carbon steel pipe inspection.

2.2. Response Surface Methodology

Response Surface Methodology (RSM) is a combination of the statistical and mathematical technique used in the engineering field for the optimization purpose. Generally, there are many designs of experiment (DOE) methods that can be used to optimize independent variables. These methods include factorial, RSM (Central Composite Design (CCD), Box-Behnken Design (BBD), Mixture, and Taguchi methods. In this finding, Central Composite Design (CCD) has been employed to create the input parameters due to the fact that CCD provides precise prediction results compare to other methods [19].

The goal of this finding is to optimize the independent parameters of GMR-BC probe design parameters. The estimation procedure of this approach is shown in Figure 1; the desired objective is the number of the axial and hole defect detection which is determined as the response. The chosen parameters that are supposed to influence the detection of the axial and hole defect are the number of GMR sensors, height of coil, and lift-off. Experiments based on probe design for each run are carried out based on the design matrix of CCD (central composite design); 20 experimental runs (N) were generated.

In order to evaluate the experimental runs needed for the three considered independent parameters, the equation provided by [20] as presented in (1) was used.

$$N = 2^{n} + 2n + n_c = 8 + 2 * 3 + 6 = 20 \quad (1)$$

where n denotes the number of independent parameters and nc is replicates of the test at the centre. For the three parameters, the suggested number of tests at the center is 6 [21].

The experimental results, depending on different parameters design, were carried out using a design matrix to obtain the corresponding responses. The ANOVA was evaluated to analyze the relationship between the factors and responses. The significant factor on the response has a p-value less than 0.05. The determination coefficient R2 was utilized to test the fitting quality. The value of R2 ranges from 0 to 1, where high values indicate the best fitting of the mathematical model with experimental observation. In case the quality of fit is not satisfactory, the design matrix will be reconstructed through the addition of more experimental runs.

Furthermore, the quadratic polynomial model was obtained and utilized to predict the performance. Subsequently, optimization was employed using desirability profile and its functions. The optimum design variables with higher desirability were selected to be the final design for the GMR-BC probe. The optimization analysis was established by the desirability analysis in (2).

$$D = (d_1 \times d_2 \times .....\times d_n)^{\frac{1}{n}} = (\prod_{i=1}^{n} d_i)^{\frac{1}{n}} \quad (2)$$

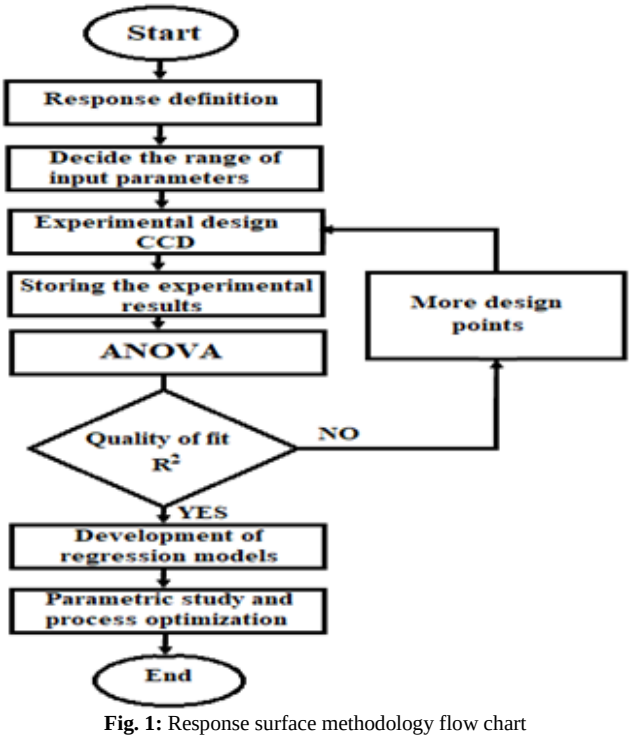

Fig. 1: Response surface methodology flow chart

3. The Proposed GMR-BC Probe

The GMR-BC probe was selected based on several factors. In ECT probe design, the excitation section and the pick-up section parameters can be varied independently to optimize their response to a defect. The GMR-BC probe operates in a hybrid mode operating using the independent excitation bobbin coil and an array of GMR sensors. There is no conjugation between the inducer and magnetic field sensor. This configuration fosters the sensitivity of a probe to

the defects. The excitation bobbin coils are winded on a shielded aluminium which centralize the magnetic field lines across the tube central axis. Thus, it minimized the leakage fields compression because of the direct magnetizing fields. The cylinder structure of a pipe will result in a varied position of individual GMR sensor in the array sensor to estimate the radial component of the induced magnetic field (Br) [22]. Therefore, the optimum sensors are required to examine the totality of an inner pipe surface. The circumferential GMR array sensor was maintained at aligned of the bobbin coils for the identification of a radial component of magnetic field leakages. The bobbin coils and GMR array sensor were transferred together as a single unit within the pipe in an axial direction with varied magnetic field due to the presence of a defect that was estimated through the array of GMR sensors. The bobbin coil induces uniform EC along θ-axis within the inner wall of carbon steel pipe. In the presence of an axial or hole defect, the EC flow is disturbed. GMR is used to carry the disturbed magnetic field. The structure of the proposed GMR-BC probe is illustrated in Figure 2.

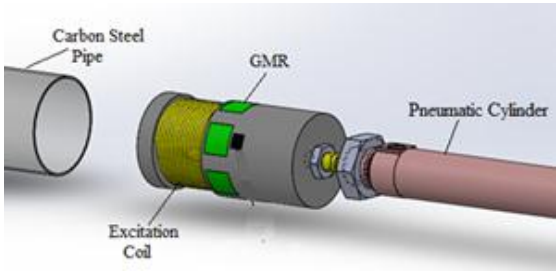

Fig. 2: A Schematic diagram of GMR-BC probe

Table 1 illustrates the selected input variables and their levels used in designing the parameters of the GMR-BC probe. In the table, (-1), (0) and (+1) indicate the lowest, central and highest levels, respectively. Three GMR-BC probe design parameters are investigated. Design parameter A is the GMR sensor in the array sensor, design parameter B is the lift-off, and the design parameter C is the height of the coil. The frequency of excitation coil for the deep penetration of eddy current is fixed at 30 kHz which is the optimum value for carbon steel material based on the previous studies [14, 22, 23]. Moreover, the responses in this study are a number of axial defects detected and a number of hole defects detected.

Table 1: Independent parameters considered in this study and their levels for central composite

Parameter	-1	0	+1
Number of GMR sensor	4	6	8
Height of coil (mm)	4	7	10
Lift-off (mm)	2	3	4

The goal was to increase the number of defect detection of the axial and hole defect in pipe defect inspection and reduce the number of GMR sensor as the height of coil and lift-off are set at a certain range for satisfactory results within the upper and lower limits. The result that has higher desirability is selected. The optimization analysis was established by the desirability analysis in (2) [24]. Table 2 presents the upper and target values for all the variable responses.

Table 2: Target value and limit for the optimized GMR-BC probe design parameters

Probe Design Parameter and Respond	Target	Lower Limit	Upper Limit
Number of GMR sensor	Minimize	4	8
Lift-off (mm)	In a range	2	4
Height of the Coil (mm)	In a range	4	10
Axial defect	Maximize	1	15
Hole defect	Maximize	1	15

4. Experimental Set-Up

4.1. Eddy Current Testing Inspection System ECTI

The schematic diagram of the testing inspection system (ECTIS) for examining the carbon steel pipeline is shown in Figure 3. It consists of five parts of development planning and enabling easy troubleshooting which includes power system, probe design, electro-pneumatic system, pipeline sample with an artificial defect, and data acquisition system and personal computer.

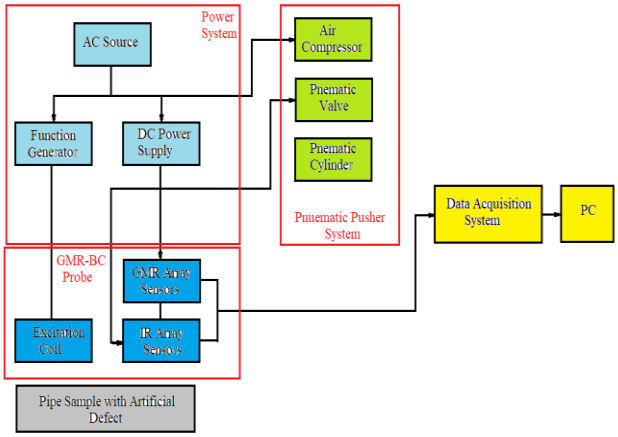

Fig. 3: Eddy Current Testing Inspection System (ECTIS)

The experimental process was evolved to evaluate the GMR-BC probe operation and optimizing its parameters to maximize defect detection probability. A GMR-BC probe prototype was developed in the laboratory to verify the numerical results, as illustrated in Figure 4. The number of GMR sensor, lift-off and height of coil are changed based on central composite design (CCD). A sinusoidal current source with an amplitude equal to 5 V used to excite the bobbin coil was the experimental result obtained at 30 kHz of frequency. Out of the two sample of carbon steel pipe, one of them has 15 axial defects of depth 5 mm (100%), length of 13.5 mm and width of 2 mm, the second sample has 15 holes defects with a diameter of 5mm and depth of 5 mm (100%). Defects in the two samples are located randomly around the circumferential direction of the pipe wall.

Fig. 4: Experimental set-up with the prototype of GMR-BC probe

The change in the GMR sensors resistance is recorded as a voltage signal; the output of the GMR sensor is scanned through Arduino Mega 2650 which possesses 54 digital pins. Each of the 54 digital I/O pins and 16 analog inputs operate at 5 volts. An individual pin can generate or acquire a maximum of 40 mA with an internal pull-up resistor (disconnected by default) of 20-50 kΩ. The output signals are displayed on a computer by MATLAB 2015 software. The result is displayed in an X-Y graph. In the X-Y graph plots, the voltage amplitude was plotted against data sampling time.

4.2. The Pipe Sample under Examination

Carbon steel comprises carbon and a steel alloy of iron. The higher quantity of carbon allows carbon steel to possess its familiar dark

colour. In this study, the pipe sample of carbon steel material that has the external and internal diameters of 55 and 50 mm, respectively was used. The electric conductivity of this material is equal to 3.18% of the International Annealed Copper Standard. Due to its shock resistance, hardness and strength, the non-ferromagnetic carbon steel are used in many industrial applications such as power plant, high-pressure fluid transportation, water mains under roads and industrial machinery, tools, and structures [25]. Several classic standard defects such as axial and hole cracks were built into the pipe sample similar to previous studies [26-28] so as to examine the defect detection using the proposed GMR-BC probe. Figure 5 illustrates two kinds of defects.

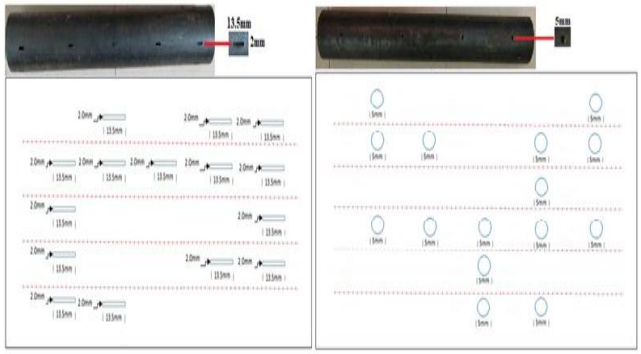

(a) (b)

Fig.5: Geometry dimension on carbon steel pipe (a) axial defect (b) hole defect

5. Results and Discussion

System's functionalities, accuracy and performance of the defects in 55 mm carbon steel pipe were evaluated by conducting the experimental tests. Data analysis of optimizing the GMR-BC probe design and the explanation of defect signals are provided and explained in the followed sections.

5.1. Statistical Analysis

RSM was employed to examine the effect of GMR-BC probe design parameters which include the lift-off, the number of GMR sensors and the height of coil to obtain the optimum performance of GMR-BC probe depending on the outcomes of axial and hole defect detection in the carbon steel pipes. The arrangement of central composite design, response, and their values from the experimental results of different GMR-BC probe design parameters were tabulated. A total number of twenty runs was conducted and the responses are listed in Table 3. Six replicates at the centre of CCD were employed to determine pure error sum of squares. Furthermore, to minimize the influence of the extraneous parameters, all the experiments were performed in randomized order [29].

Table 3: Central composite design matrix, response and their values for experimental results of axial and hole defect in carbon steel pipe

	Independent Factors			Response	
Run	Number GMR Sensor	Lift-Off (mm)	Height of Coil (mm)	Axial Defect Detect	Hole Defect Detect
1	8	3	7.	8	7
2	4	3	7	3	1
3	6	2	7	10	8
4	8	4	10	9	9
5	4	2	4	4	1
6	4	4	10	4	4
7	4.	4	4	1	1
8	6	4	7	5	5
9	8	4	4	5	6
10	6	3	7	7	5
11	6	3	7	7	5
12	6	3	10	10	9
13	8	2	4	9	9
14	6	3	7	7	5
15	6	3	4	6	5
16	8	2	10	15	15
17	6	3	7	7	5
18	4	2	10	6	6
19	6	3	7	7	5
20	6.00	3	7	7	5

The ANOVA results illustrated the significant terms in the proposed model as presented in Tables 3 and 4. The F-value for axial and hole defect detect are 112.94 and 252.88 respectively. This indicated that the empirical model is significant in the prediction of a defect in the pipe inspection by utilizing this ECTI system. For a significant model term, the value of Prob-F must be less than 0.05. Therefore, this ensures that the empirical model reflects the system and fit to predict the response. In case the Prob F is greater than 0.1000, this shows that the model term is not significant. Regression analysis and normality were carried out to verify the model accuracy in the prediction of the defect in pipe inspection based on difference ECT probe parameter designs. After these tests had been successfully carried out, the significance of the model is ascertained whereby a mathematical model equation that shows the relationship between the defect detection rate in the inspected pipe and ECT probe design variables is derived.

5.2. Axial Defect

Design expert software was employed to study the effect of independent parameters on the responses. Experimental results reflected that the number of axial and hole defect detection varied between (3-15) and (1-15), respectively. From Table 4, the total determination R2 is 98.50 % which is closer to 1, this indicated that the quadratic model significantly fit the experimental data and will be good in representing axial defect detection in relative to the independent variables [29, 30]. Using t-test and p-value, the significance of each variable was evaluated ($p < 0.05$).

Table 4 shows the analysis of variance (ANOVA) of all the independent variables, the number of GMR sensors, a height of the coil, and lift-off were significant ($p < 0.05$). Additionally, the interaction impact of the height of the coil and lift-off was insignificant as the p-value was equal to 0.4673. Thus, any insignificant term was removed, and the optimization process was repeated until all the terms are significant.

Table 4: ANOVA table for axial defect detection response surface quadratic model

Source	Sum of Squares	df	Mean Square	F value	p-Value
Model	168.00	7	24.00	112.94	< 0.0001
A-Nu sensor	78.40	1	78.40	368.94	< 0.0001
B-Lift-off	40.00	1	40.00	188.24	< 0.0001
C-Height of Coil	36.10	1	36.10	169.88	< 0.0001
AB	3.12	1	3.12	14.71	0.0024
AC	3.13	1	3.13	14.71	0.0024
A2	7.20	1	7.20	33.88	< 0.0001
C2	3.20	1	3.20	15.06	0.0022
Residual	2.55	12	0.21		
Lack of Fit	2.55	7	0.36		
Pure Error	0.000	5	0.000		
Cor Total	170.55	19			

The yield estimated regression coefficients for axial defect for the quadratic equation with ''Pred. R2" of 0.9143 is in a good relationship with the ''Adj. R2" of 0.9763 with a difference of < 0.2. The implementation of the results followed the regression equation (4) which can be taken as an interaction between the number of axial defect and the independent parameters.

$$f(axial) = -6.40098 + 6.10833A - 0.12500B - 1.54722C - 0.31250AB + 0.10417AC - 0.37500A^2 + 0.11111C^2 \quad (3)$$

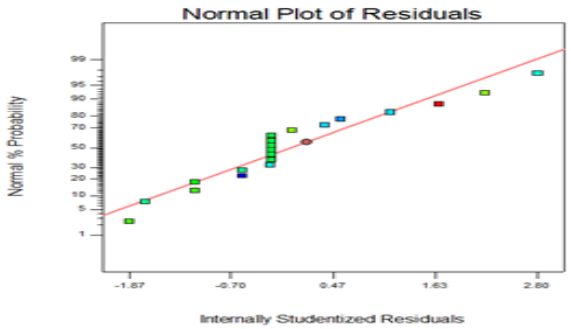

Fig. 6: Normal probability plot for axial defect detection

The residual plots for the number of axial defect detection are essential to evaluate the validity of a model. Figure 6 displays the normal probability plot for the residual distributions which is an additional validation for the response surface methodology model [31]. It can be clearly observed from the figure that the normal probability diagram for axial defect detection is very close to a straight-line and there is no evidence of an outlier. This indicates that the errors are normally distributed and the full quadratic regression equation is exceedingly fitted to the observed data [30].

5.3. Hole Defect

Table 5 provides the estimated coefficients for the quadratic model of hole defect detection in the inspection of carbon steel pipe.. Table 6 indicates that the estimated coefficients of the remaining terms after eliminating the non-significant terms. The value of the R2 is equal to 99.46 %. Therefore, the model can represent the response of hole defect detection in terms of the investigated parameters. The interaction impact of the number of GMR sensor and the height of coil has a p-value of > 0.05.

Table 5: Estimated regression coefficients for hole defect detection for quadratic equation

Source	Sum of Squares	df	Mean Square	F Value	p-Value
Model	198.25	9	23.03	231.32	< 0.0001
A-Nu sensor	108.90	1	108.90	1143.58	< 0.0001
B-Lift-off	19.60	1	19.60	205.82	< 0.0001
C-Height of Coil	44.10	1	44.10	463.10	< 0.0001
AB	6.12	1	6.12	64.32	< 0.0001
AC	0.13	1	0.13	1.31	0.2786
BC	3.12	1	3.12	32.82	0.0002
A2	5.46	1	5.46	57.34	< 0.0001
B2	3.27	1	3.27	34.37	0.0002
C2	6.96	1	6.96	73.09	< 0.0001
Residual	0.95	10	0.095		
Lack of Fit	0.95	5	0.19		
Pure Error	0.000	5	0.000		
Cor Total	199.20	19			

R2 = 99.52 %; R2 (adj.) = 99.09%; R2 (adj.) = 96.30%

Table 6: ANOVA for estimated regression coefficients for hole defect detection for quadratic equation after the elimination of non-significant terms

Source	Sum of Squares	df	Mean Square	F Value	p-Value
Model	198.12	8	24.77	252.88	< 0.0001
A-Nu sensor	108.90	1	108.90	1111.97	< 0.0001
B-Lift-off	19.60	1	19.60	200.14	< 0.0001
C-Height of Coil	44.10	1	44.10	450.30	< 0.0001
AB	6.12	1	6.12	62.54	< 0.0001
BC	3.12	1	3.12	31.91	< 0.0001
A2	5.46	1	5.46	55.75	< 0.0001
B2	3.27	1	3.27	33.42	< 0.0001
C2	6.96	1	6.96	71.07	0.0001
Residual	1.08	11	0.098		
Lack of Fit	1.08	6	0.18		
Pure Error	0.000	5	0.000		
Cor Total	199.20	19			

R2 = 99.46 %, R2 (adj.) = 99.07%; R2 (Pred.) = 97.24%

Figure 7 reveals that the normal probability plot is a straight line. The following quadratic equations present the correlation between the independent variables and the response hole defect detection.

$$f(hole) = -9.37820 + 7.18977A - 3.86212B - 1.14975C - 0.43750AB - 0.20833BC - 0.35227A^2 + 1.09091B^2 + 0.17677C^2 \quad (4)$$

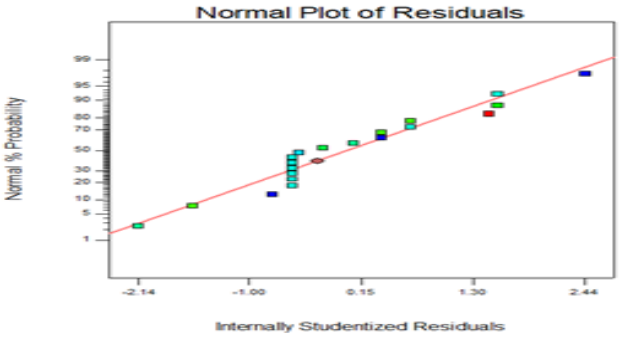

Fig.7: Normal probability plot for hole defect

It is clearly observed that the relationship between probe variable designs influences the hole defect detection variance. Figure 8 illustrates the relationship between the variables that involve GMR sensors, lift-off and hole defect detection. Thus, the probe design variables are taken into consideration for the optimization of hole defect detection.

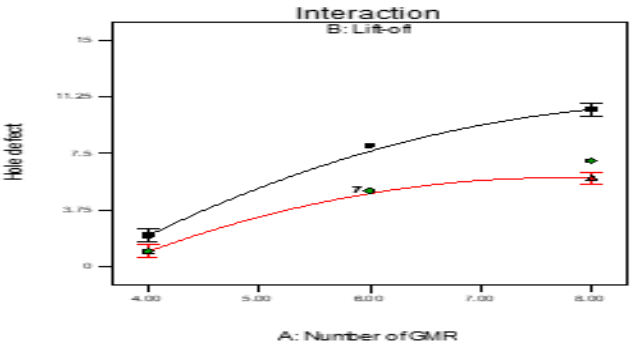

Fig. 8: The interaction between probe diameter and the number of GMR sensor on hole defect detection (height of Coil = 10.00 mm)

The relationship between the predicted data of defect detection by utilizing the empirical model and the actual experimental data of defect detection using GMR-BC probe are shown in Figures 9 a-b. The experimental and predicted observations were close to each other, showing a good regression. The predicted values matched with the experimental data points, indicating a good fitness, with an R2 value of 0.9850 at axial defect and an R2 value of 0.9946 at hole defect. So, with the relationships in (4)-(5), the response (defect detection) at any point within the range of the experimental interval could be predicted.

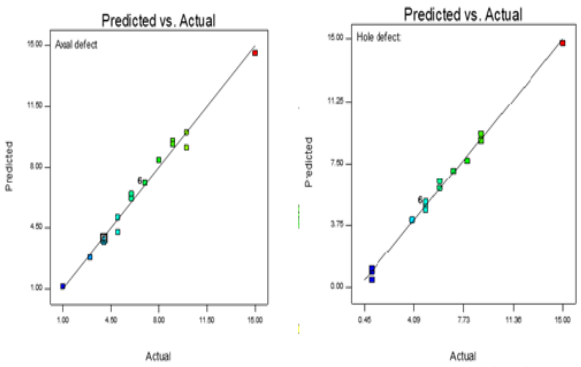

Fig. 9: Relation between experimental and predicted values of defect detection at (a) axial defect detection (b) hole defect detection

5.4. Optimization Parameters of the Probe Design

Figure 10 shows the response optimization plot for the effect of the number of GMR sensors, lift-off, and height of coil on both responses. The optimum condition for all case studies was achieved when the axial and hole defect detection is maximized with the highest desirability value of 0.679. From the figure, the RSM result showed that the axial and hole defect detection is maximized as the ECT probe designed parameter is 6 GMR sensor utilized for the array sensor, the lift-off is 2mm (probe diameter = 51 mm), and the height of coil is 10 mm. Comparing these results with literature findings, the 6 optimum GMR sensor is in agreement with previous studies [8].

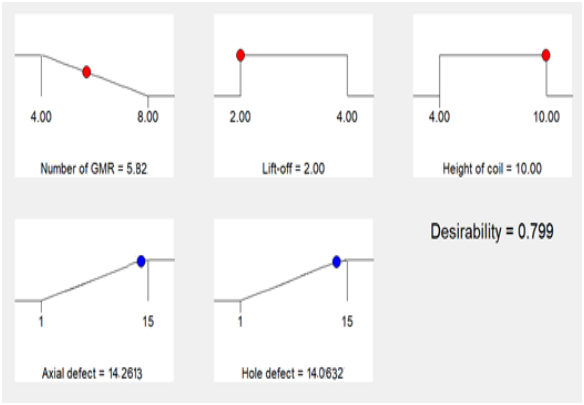

Fig. 10: Response optimization plot for axial and hole defect detection

The 3-D surface and 2-D contour plots reflect an effect of the relationship between two variables of the axial and hole defect detection under optimum GMR-BC probe design parameter. The impacts of the independent parameters on the responses are illustrated graphically using contour plots and 3D surface plots. These graphs were drawn by fixing one independent parameter while the other two parameters determine the yields. From Figure 11, it can be observed that increasing the height of coil and decreasing lift-off, defect detection increase. This might be due to the fact that increasing height of coil and decreasing lift-off, the intensity of eddy current in the conductive material is increases [4].

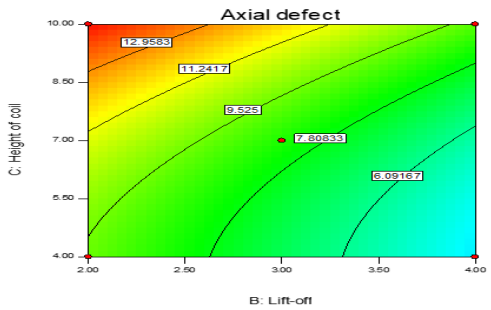

(a)

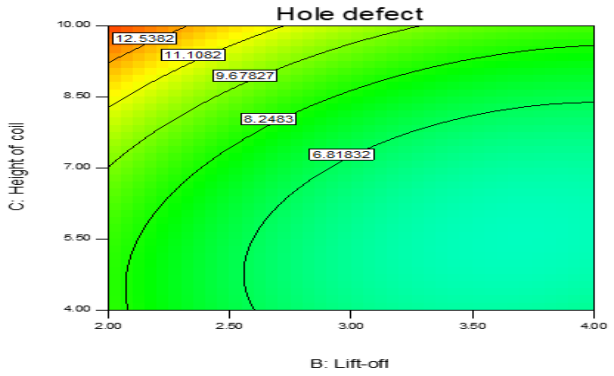

(b)

Fig. 11: Variation of (a) axial defect detection and (b) hole defect detection against the height of coil and lift-off

The 3D surface graphical plots present the effect of the relationship between two variables. Two sets of correlation which include AB and AC for the response of axial defect detection, while AB and BC for the response of hole defect detection were observed. Figure 12 (a) shows the axial defect detection against AB; it revealed a linear effect of the lift-off and quadratic effect of GMR sensors on the axial defect detection. Figure 12 (b) shows hole defect detection against BC; the graph shows that decreasing the lift-off has a slight effect on the response, while the height of a coil showed a significant increasing trend for hole defect detection. Therefore, from the above discussion for defect detection, the optimum design is obtained with the highest height of coil and lowest lift-off.

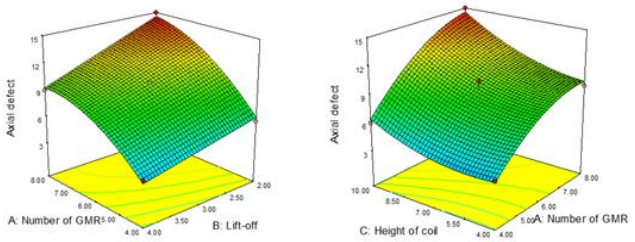

(a)

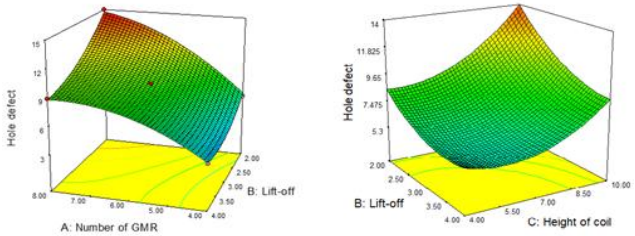

(b)

Fig. 12: Response surface plots for (a) axial defect detection against AB and AC and (b) hole defect detection against AB and BC

6. Experimental Results for Axial and Hole defect

The GMR-BC probe generates an eddy current in the pipe wall and needs to be scanned across the axial direction of pipe for defect detection in a pipe wall. Thus, the GMR-BC probe possesses a higher sensitivity to the different type of defects, such as axial and hole notches. The GMR-BC probe with optimum parameters obtain from RSM optimization were utilized and tested for defect detection in the carbon steel pipe as illustrated in Figure 13. The GMR-BC probe designed parameter is the 6 GMR sensors utilized in the sensor array, coil thickness is 10 mm, and probe diameter is 51 mm.

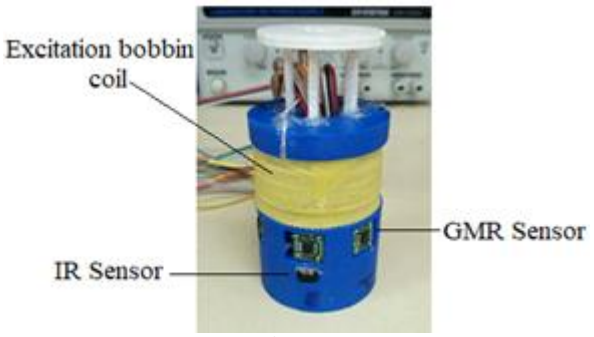

Fig. 13: GMR-BC Probe Design of ECTI System Based on Optimum Variable Design

The axial and hole defect on carbon steel pipe is fabricated using electrical discharge machining (EDM). Size dimension of defect axial defect is a width of 2.0 mm, a height of 13.5 mm, and diameter of hole defect is 5 mm. The GMR sensor array has a self-nulling property and produces a nearly constant voltage level (flat curves) without defect. The GMR signal is generated in a larger amount through axial component; magnetic field can occur if a defect is present in the pipe wall. The closer the sensors to a pipe, the more the variation in resistance (or output voltage). The sensor waveform could be sine-like waveform or spike or pulse waveform, showing varied defects with different orientation, shape or size to ensure that the detectors move to the remote zone. The equidistance that exists between the detector and excitation coil was selected to be 3 mm [26]. For examination purpose, an axial and hole defect of 5 mm in depth and 100% of the tube wall were examined by utilizing the experimental set-up of GMR-BC probe. A sinusoidal current with an amplitude of 5 V and a current excitation frequency of 30 kHz was used on the excitation coil. The first experimental observation was carried out by moving the GMR-BC probe across the sample inner tube wall with 15 axial defects. The second test was a scanning sample with 15 holes defects and the GMR-BC probe. The output amplitudes of GMR sensor array in GMR-BC probe for both experimental are depicted in Figures 14 and 15.

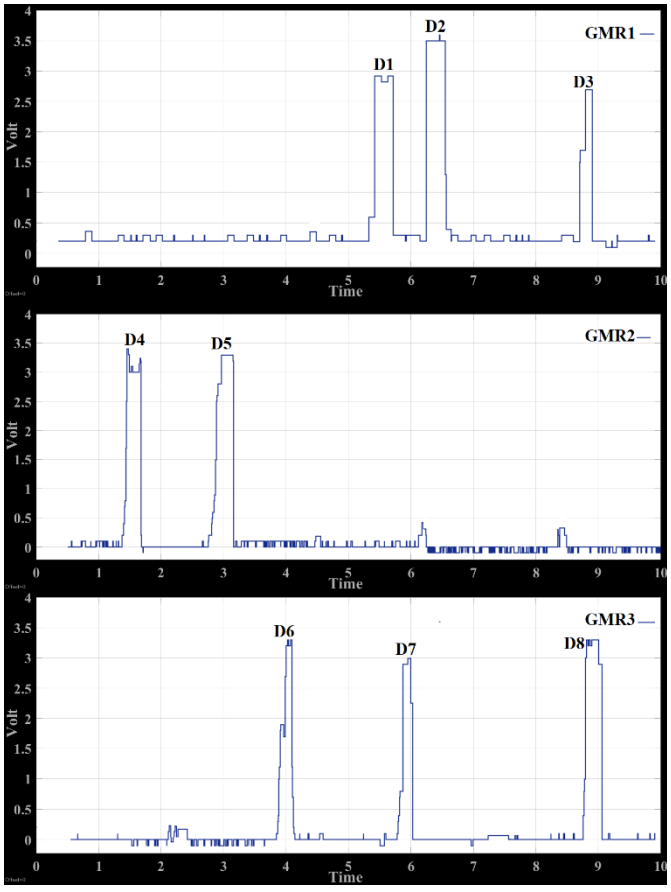

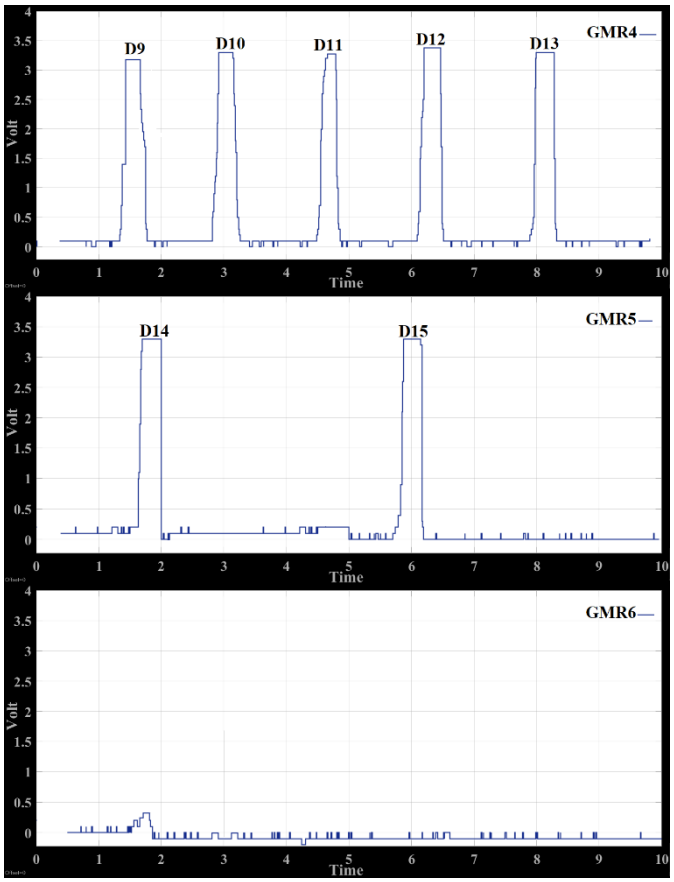

Fig. 14: The axial crack detection test result

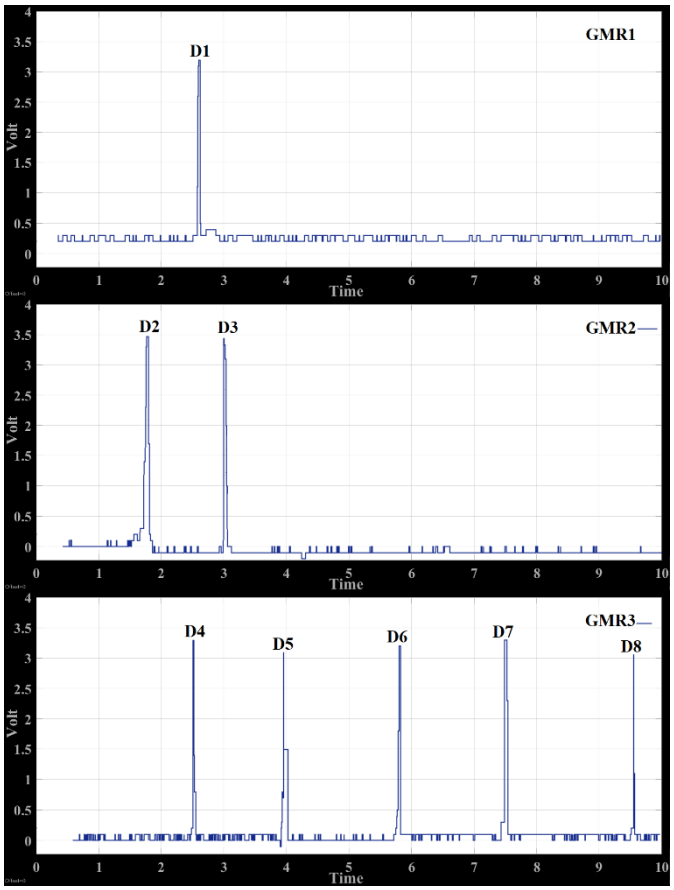

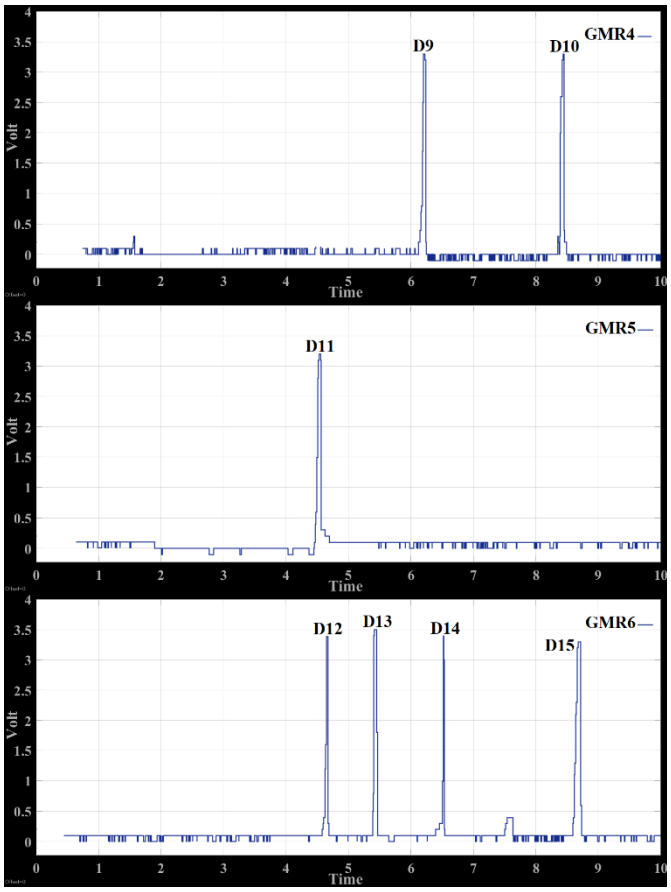

Fig. 15: The hole crack detection test result

It can be observed in the results that both axial and hole notches are detected experimentally through the prototype GMR-BC probe. The magnitudes of axial and hole defect signals comparably indicate that the probe possesses similar sensitivity to axial and hole defect. The detection rate for both types of the defect is high, giving 100%.

Detailed analysis of the defect signal for the axial and hole shows that the signal generated through axial defect has a signal width which is larger compared to the signal defect generated through a hole defect. This indicates that different sizes of defect were generated by different signal profiles and this is useful for defect classification. The variation in peak amplitude of signal across the defect can be utilized in classifying surface and subsurface defects. This finding focused on early detection of defects; nevertheless, an examination of depth defect through peak amplitude is affected through defect depth and lift-off. More extensive experiments are currently carried out to increase the performance of probe in terms of accuracy with respect to probe lift-off variation.

7. Conclusion

The GMR-BC probe for pipe defect detection was fabricated, developed, and analysed in this study. The bobbin coil was used to excite the material and GMR sensor array was used as a detector to pick up the magnetic field. The response surface methodology was used to optimize GMR-BC probe design for maximizing defect detection probability. Six GMR sensor arrays, lift-off of 2 mm, and a coil height of 10 mm were the optimal parameters for maxi-mum defect detection in 55 mm carbon steel pipe inspection. The GMR sensor has a self-nulling characteristic and pick-up changes in an axial component of a magnetic field. The GMR-BC probe can detect axial and hole defects in carbon steel pipes.

Acknowledgement

We will like to thank UMP for supporting this study through the RDU 170379 grant.

References

[1] T. El-Shiekh, "Leak detection methods in transmission pipelines," Energy Sources, Part A: Recovery, Utilization, and Environmental Effects, 32, 715-726, 2010.
[2] W. Du, H. Nguyen, A. Dutt, and K. Scallion, "Design of a GMR sensor array system for robotic pipe inspection," Proceedings of the IEEE Sensors, 2010, pp. 2551-2554.
[3] I. Abidin, M. Umar, M. Yusof, M. Ibrahim, A. Hamzah, and M. Salleh, "Advantages and applications of Eddy current thermography testing for comprehensive and reliable defect assessment," Proceedings of the 18th World Conference on Nondestructive Testing, Durban, South Africa, 2012, pp. 16-20.
[4] J. Garcia-Martin, J. Gomez-Gil, and E. Vazquez-Sanchez, "Non-destructive techniques based on Eddy current testing," Sensors, 11, 2525-2565, 2011.
[5] M. A. Faraj, F. Samsuri, and A. N. AbdAlla, "Hybrid of Eddy current probe based on permanent magnet and GMR sensor," Journal of Telecommunication, Electronic and Computer Engineering, 10, 7-11, 2018.
[6] J. Bailey, N. Long, and A. Hunze, "Eddy current testing with Giant Magnetoresistance (GMR) sensors and a pipe-encircling excitation for evaluation of corrosion under insulation," Sensors, 17, 1-21, 2017.
[7] M. Kaack, T. Orth, G. Fischer, W. Weingarten, S. Koka, and N. Arzt, "Application of GMR sensors for the industrial inspection of seamless steel pipes," Proceedings of the 11th Symposium on Magnetoresistive Sensors and Magnetic Systems, 2011, pp. 29-30.
[8] W. Cheng, "Pulsed eddy current testing of carbon steel pipes' wall-thinning through insulation and cladding," Journal of Nondestructive evaluation, 31, 215-224, 2012.
[9] D. Rifai, A. N. Abdalla, R. Razali, K. Ali, and M. A. Faraj, "An Eddy current testing platform system for pipe defect inspection based on an optimized Eddy current technique probe design," Sensors, 17, 1-24, 2017.
[10] K. Tsukada, M. Hayashi, Y. Nakamura, K. Sakai, and T. Kiwa, "Small Eddy current testing sensor probe using a tunneling magnetoresistance sensor to detect cracks in steel structures," IEEE Transactions on Magnetics, 2018, 1-5, 2018.
[11] B. Sasi, V. Arjun, C. Mukhopadhyay, and B. Rao, "Enhanced detection of deep seated flaws in 316 stainless steel plates using integrated EC-GMR sensor," Sensors and Actuators A: Physical, 275, 44-50, 2018.
[12] J.-T. Jeng, G.-S. Lee, W.-C. Liao, and C.-L. Shu, "Depth-resolved Eddy-current detection with GMR magnetometer," Journal of Magnetism and Magnetic Materials, 304, e470-e473, 2006.
[13] D. Pasadas, A. L. Ribeiro, T. Rocha, and H. G. Ramos, "Open crack depth evaluation using eddy current methods and GMR detection," Proceedings of the IEEE Metrology for Aerospace, 2014, pp. 117-121.
[14] J. Xin, N. Lei, L. Udpa, and S. S. Udpa, "Rotating field eddy current probe with bobbin pickup coil for steam generator tubes inspection," Ndt & E International, 54, 45-55, 2013.
[15] L. S. Rosado, J. C. Gonzalez, T. G. Santos, P. M. Ramos, and M. Piedade, "Geometric optimization of a differential planar eddy currents probe for non-destructive testing," Sensors and Actuators A: Physical, 197, 96-105, 2013.
[16] M. Li and D. Lowther, "NDT sensor design optimization for accurate crack reconstruction," COMPEL-International Journal for Computation and Mathematics in Electrical and Electronic Engineering, 31, 792-802, 2012.
[17] X. A. Yuan, W. Li, G. Chen, X. Yin, J. Ge, W. Jiang, and J. Zhao, "Bobbin coil probe with sensor arrays for imaging and evaluation of longitudinal cracks inside aluminum tubes," IEEE Sensors Journal, 2018, 1-8, 2018.
[18] W. S. Singh, B. P. Rao, S. Thirunavukkarasu, S. Mahadevan, C. Mukhopadhyay, and T. Jayakumar, "Development of magnetic flux leakage technique for examination of steam generator tubes of prototype fast breeder reactor," Annals of Nuclear Energy, 83, 57-64, 2015.
[19] M. Kaushal, P. Dhiman, S. Singh, and H. Patel, "Finite volume and response surface methodology based performance prediction and optimization of a hybrid earth to air tunnel heat exchanger," Energy and Buildings, 104, 25-35, 2015.

[20] J. Sahu, J. Acharya, and B. Meikap, "Response surface modeling and optimization of chromium (VI) removal from aqueous solution using Tamarind wood activated carbon in batch process," Journal of hazardous materials, 172, 818-825, 2009.
[21] G. E. Box and J. S. Hunter, "The 2 k—p fractional factorial designs," Technometrics, 3, 311-351, 1961.
[22] C. Ye, Y. Huang, L. Udpa, and S. S. Udpa, "Novel rotating current probe with GMR array sensors for steam generate tube inspection," IEEE Sensors Journal, 16, 4995-5002, 2016.
[23] J. Paw, K. Ali, C. Hen, A. Abdallah, T. Ding, N. Ahlam, and N. Eirfan, "Encircling probe with multi-excitation frequency signal for depth crack defect in Eddy current testing," Journal of Fundamental and Applied Sciences, 10, 949-964, 2018.
[24] S. Ghafari, H. A. Aziz, M. H. Isa, and A. A. Zinatizadeh, "Application of response surface methodology (RSM) to optimize coagulation–flocculation treatment of leachate using poly-aluminum chloride (PAC) and alum," Journal of hazardous materials, 163, 650-656, 2009.
[25] N. S. El-Gendy, A. Hamdy, and B. A. Omran, "Thermal and surface studies on the corrosion inhibition of petroleum pipeline by aqueous extract of Allium cepa skin under acidic condition," Energy Sources, Part A: Recovery, Utilization, and Environmental Effects, 40, 905-915, 2018.
[26] A. L. Ribeiro, A. L. Ribeiro, H. G. Ramos, and T. J. Rocha, "Defect detection in stainless steel tubes with AMR and GMR sensors using remote field Eddy current inspection," ACTA IMEKO, 4, 62-67, 2015.
[27] W. S. Singh, B. P. Rao, C. Mukhopadhyay, and T. Jayakumar, "Detection of localized damage in water wall tubes of thermal power plants using GMR sensor array based magnetic flux leakage technique," Journal of Nondestructive Evaluation, 34, 1-7, 2015.
[28] V. Suresh, A. Abudhahir, and J. Daniel, "Development of magnetic flux leakage measuring system for detection of defect in small diameter steam generator tube," Measurement, 95, 273-279, 2017.
[29] E. Firatligil-Durmus and O. Evranuz, "Response surface methodology for protein extraction optimization of red pepper seed (Capsicum frutescens)," LWT-Food Science and Technology, 43, 226-231, 2010.
[30] H. Joardar, N. Das, and G. Sutradhar, "An experimental study of effect of process parameters in turning of LM6/SiC P metal matrix composite and its prediction using response surface methodology," International Journal of Engineering, Science and Technology, 3, 132-141, 2011.
[31] S. Rashidi, M. Bovand, and J. Esfahani, "Heat transfer enhancement and pressure drop penalty in porous solar heat exchangers: A sensitivity analysis," Energy Conversion and Management, 103, 726-738, 2015.